Comparison of two cluster-expansion methods for the energetics of Pd-V alloys

C. Wolverton and Alex Zunger
National Renewable Energy Laboratory, Golden, Colorado 80401
(Received 22 February 1994)

The formation energies of substitutional transition-metal alloys are examined by several means. First, two types of direct total-energy calculations are considered, namely, (i) the local-density approximation (LDA), and (ii) a tight-binding (TB) approximation thereof. Second, these directly calculated total energies are used to construct two Ising-like cluster expansions that, if sufficiently accurate, could be used to construct the full statistical mechanics of transition-metal alloys. These are (a) the Connolly-Williams (CW) method, and (b) direct configurational averaging (DCA). Finally, the ability of these two cluster expansions [(a) and (b)] to fit and predict a large number of the underlying directly calculated [(i) and (ii)] total energies is tested, by the average prediction error χ. These tests are performed for a large number of Pd-V alloys, and also to a more limited extent, for the Pd-Rh, Pd-Ti, and Pt-V systems. We find for Pd-V that (i) direct TB calculations show significant overbinding (too-negative formation energies) relative to the LDA, with average error of χ=112 meV/atom (a typical formation energy of $Pd_{0.50}V_{0.50}$ is ~ -250 meV/atom); (ii) the CW cluster expansion mimics quite well the results of the respective direct calculations, whether LDA (χ=19 meV/atom) or TB (χ=19 meV/atom); (iii) the DCA cluster expansions provides a less accurate depiction of the TB energies on which it is based (χ=65 meV/atom); (iv) the prediction errors for the equimolar random alloys are significantly larger using the DCA than using the CW method. In light of (i) above, it appears that the tight-binding model needs to be refined before it can be used systematically for (either DCA or CW) cluster expansions.

I. INTRODUCTION: CLUSTER EXPANSIONS OF TOTAL ENERGIES

Many problems in condensed matter physics require calculations of the total energies of a large number of substitutional structures. Examples include the search for the lowest energy $T = 0$ structures among the 2^N configurations that can be made by occupying each of the N lattice sites by either an A or a B atom,[1–4] the calculation of the $T \neq 0$ composition-temperature phase diagrams of alloys,[5–15] the comparison of the relative stabilities of structural polytypes,[16–18] or differently oriented superlattices,[19] and the calculation of formation energies of random alloys,[1,4,10,11,13–15,20] substitutional impurities,[21–23] or antiphase boundaries.[24–27] *Direct*, first-principles quantum-mechanical calculations,

$$E_{\text{direct}}(\sigma) = \langle \Psi | \hat{H} | \Psi \rangle / \langle \Psi | \Psi \rangle, \tag{1}$$

are usually limited to a small number of configurations σ; the current N^3 scaling of the computational effort involved in such approaches[28] also limits the search to relatively simple, periodic structures with $\lesssim$100 atoms per computational unit cell. To overcome these limitations, one possible strategy is to retain the rigor of first-principles calculations but find computational schemes that reduce the scaling of the effort from[29] N^3 to N^2 or even[30–32] to N^1. These highly promising approaches are still in their formative stages. A popular alternative is to replace first-principles strategies by computationally much faster higher- (i.e., second-, third-) principles schemes, e.g., semiempirical or empirical approaches.

Whether one uses first-principles or other methods, however, explicit calculations of all relevant $E_{\text{direct}}(\sigma)$ would be wasteful *if* there were some inherent linear dependences among different configurational energies. A systematic method of identifying such possible dependences is the "cluster expansion" (CE) of $\{E_{\text{direct}}(\sigma)\}$ in terms of "lattice figures".[33,34] In the cluster expansion, one selects a single, underlying parent lattice (e.g., fcc, bcc, hcp) and defines a configuration σ by specifying the occupations of each of the N lattice sites by an A atom or a B atom. (If necessary, the process may be repeated for other parent lattices, e.g., fcc, bcc, hcp.) For each configuration, one assigns a set of spin variables, $\hat{S}_i$ $(i = 1, 2, ..., N)$ to each of the N sites with $\hat{S}_i = -1$ or $+1$ if site i is occupied by an A or B atom, respectively. The problem of finding the energy of the 2^N possible configurations σ can be *exactly*[35–37] mapped onto a generalized Ising Hamiltonian

$$E_{\text{CE}}(\sigma) = J_0 + \sum_i J_i \hat{S}_i(\sigma) + \sum_{j<i} J_{ij} \hat{S}_i(\sigma) \hat{S}_j(\sigma) + \sum_{k<j<i} J_{ijk} \hat{S}_i(\sigma) \hat{S}_j(\sigma) \hat{S}_k(\sigma) + \cdots, \tag{2}$$

where the J's are the interaction energies ("effective cluster interactions") and the first summation is over all sites in the lattice, the second over all pairs of sites, the third over all triplets, and so on. The interaction energies possess the symmetry properties of the parent lattice, and thus, all terms with equal coefficients in (2) may be

grouped together. Consequently, Eq. (2) can be written more compactly as

$$E_{\rm CE}(\sigma) = \sum_f D_f \, J_f \, \overline{\Pi}_f(\sigma) \ , \tag{3}$$

where f is a symmetry-distinct figure comprised of several lattice sites (pairs, triplets, etc.), D_f is the number of figures per lattice site, J_f is the Ising-like interaction for the figure f, and the "lattice-averaged product" $\overline{\Pi}_f$ is defined as a product of the variables $\hat{S}_i$, over all sites of the figure f with the overbar denoting an average over all symmetry equivalent figures of lattice sites

$$\overline{\Pi}_f(\sigma) = \frac{1}{N_L} \sum_{\hat{R}}^{N_L} \Pi_{\hat{R}f}(\sigma) \ , \tag{4}$$

where the summation is over the N_L space group operations ($\hat{R}$) of the *lattice*. The completeness and orthonormality of the set $\{\Pi_f(\sigma)\}$ of spin products[35] in the space of all configurations assures that expansions (2) and (3) are exact if all 2^N figures are used to describe all 2^N configurational energies. The exact, rigorous nature of the expansions is true whether or not atoms relax off their nominal lattice sites, since the relaxed energy is a unique function of the unrelaxed configuration.

While mathematical completeness requires that all 2^N terms be included in Eqs. (2) and (3), physical intuition suggests that some interactions are less important than others, and thus could be neglected. *If* one can determine that $N_F \ll 2^N$ interactions are important, one could calculate *directly* (i.e., independently of the CE) the total energies of N_σ structures and obtain the set of $\{J_f\}$ by singular value decomposition[11,14]

$$\sum_\sigma^{N_\sigma} \left| \sum_f^{N_F} D_f \, J_f^{\rm CW} \, \overline{\Pi}_f(\sigma) - E_{\rm direct}(\sigma) \right|^2 = \min. \tag{5}$$

When $N_\sigma = N_F$, one could use matrix inversion

$$J_f^{\rm CW} = \frac{1}{D_f} \sum_\sigma^{N_\sigma} [\tilde{\overline{\Pi}}^{-1}]_{\sigma,f} \, E_{\rm direct}(\sigma) \tag{6}$$

as suggested by Connolly and Williams (CW).[38] In Eq. (6), $\tilde{\overline{\Pi}}$ represents the (square) $N_\sigma \times N_F$ matrix with elements $\overline{\Pi}_f(\sigma)$, and $[\tilde{\overline{\Pi}}^{-1}]_{\sigma,f}$ is the (σ, f) element of its inverse. In this manner, the set of $\{J_f\}$ is obtained simultaneously from the set of calculated energies, $\{E_{\rm direct}(\sigma)\}$, and thus, the interaction energies for two distinct figures are not independent of one another.

Alternatively, due to the orthonormality of the set of spin products of Eq. (3), one can "integrate out" the J_f one-by-one (i.e., completely independently of one another) in a manner analogous to obtaining the coefficient of a Fourier expansion from the real-space function

$$J_f^{\rm DCA} = \frac{1}{N_\sigma} \sum_\sigma^{N_\sigma} \Pi_f(\sigma) E_{\rm direct}(\sigma) \ . \tag{7}$$

Equation (7) is used in the method of direct configurational averaging (DCA).[39] In the DCA, the configurations used are determined by randomly distributing A and B atoms over the N lattice sites, with N typically being $\gtrsim 1000$. When f represents a pair of lattice sites, i and j, Eq. (7) reduces to the familiar form

$$J_{\rm ij} = \tfrac{1}{4}[\langle E_{AA}\rangle + \langle E_{BB}\rangle - \langle E_{AB}\rangle - \langle E_{BA}\rangle] \ , \tag{8}$$

where $\langle E_{AB}\rangle$ represents the average energy of all configurations chosen completely at random, with one caveat: An A-B pair of atoms is located at sites i and j. Similar definitions apply for $\langle E_{AA}\rangle$, $\langle E_{BB}\rangle$, and $\langle E_{BA}\rangle$. It should be noted that Eq. (6) is *exact* if $N_\sigma = N_F = 2^N$, whereas Eq. (7) is *exact* when $N_\sigma = 2^N$, independent of f. In what follows, we will examine the ability of the CW method [Eq. (6)] and the DCA method [Eq. (7)] to predict configurational energies when $(N_\sigma, N_F) \ll 2^N$ terms are used.

If a hierarchy of interactions exists such that $N_F \ll 2^N$ interactions can describe $E_{\rm CE}(\sigma)$ [Eq. (3)] with useful precision (i.e., that underlying the calculation of $E_{\rm direct}$), then the energy of any of the 2^N configurations can be calculated almost immediately by calculating the spin products and summing Eq. (3). Thus, after an initial investment of calculating N_σ total energies $\{E_{\rm direct}(\sigma)\}$, one could predict the energy $E(\sigma')$ of any of the remaining $2^N - N_\sigma \simeq 2^N$ configurations including structures with thousands of transition-metal atoms per unit cell[40–42] from

$$E_{\rm CE}(\sigma') = \sum_\sigma^{N_\sigma} A(\sigma, \sigma') E_{\rm direct}(\sigma) \ , \tag{9}$$

where

$$A^{\rm CW}(\sigma, \sigma') = \sum_f^{N_F} \overline{\Pi}_f(\sigma') \, [\tilde{\overline{\Pi}}^{-1}]_{\sigma,f} \tag{10}$$

if Eq. (6) is used, or

$$A^{\rm DCA}(\sigma, \sigma') = \frac{1}{N_\sigma} \sum_f^{N_F} \Pi_f(\sigma') \Pi_f(\sigma) \tag{11}$$

if Eq. (7) is used.[43] The validity of the series truncation can then be examined by contrasting the recalculated energy $E_{\rm CE}(\sigma')$ (for configurations σ' *not used* in determining $\{J_f\}$) with the directly calculated energies $E_{\rm direct}(\sigma')$. The predictive error of the CE,

$$\delta E = |E_{\rm direct}(\sigma') - E_{\rm CE}(\sigma')| \tag{12}$$

can be minimized by adding more interactions and directly calculated structures to the CE of Eq. (3). *Equation (9) then establishes the existence of approximate (i.e., within a tolerance, δE) linear dependences among the energies of different configurations.* A *converged* cluster expansion within a prescribed tolerance δE can then be used to obtain the energy of *any* of the 2^N possible configurations, at virtually no computational cost whatsoever (i.e., the calculation does not scale with any power of N, and has an enormously small prefactor). Thus, with such a CE, it is possible to determine ground state stability, composition-temperature phase diagrams, relative stabilities of structural polytypes and differently oriented superlattices, as well as formation energies of ran-

dom alloys, impurities, and antiphase boundaries. When using a CE, it is, therefore, imperative to examine its ability to produce reasonable predictive errors [Eq. (12)].

II. ACCURACY ISSUES IN THE DCA AND CW METHODS

The efficacy of the aforementioned approaches depends on several factors, which may be grouped into two broad categories:

(1) *The accuracy with which the input* $E_{\rm direct}(\sigma)$ *is computed.* In the DCA method, the configurations used to determine J_f [Eq. (7)] have *random* occupations of the N sites and as many as 1500 sites per configuration. This large number of atoms currently precludes the use of accurate first-principles techniques to calculate $E_{\rm direct}(\sigma)$. On the other hand, in the CW method one assumes at the outset that only N_F figures are retained, so practically any[44] $N_\sigma \geq N_F$ configurations will do for the purpose of calculating J_f [Eq. (6)]. One thus selects the most convenient ones: configurations that correspond to various *periodic, ordered structures.* Thus, first-principles local-density approximation (LDA) methods are readily applicable.

(2) *The accuracy of the recalculated configurational energies* $E_{\rm CE}(\sigma')$ [Eq. (9)] *with respect to* $E_{\rm direct}(\sigma')$. This ultimate test examines *all* convergence issues simultaneously: the truncation to N_f figures *as the first step* in the CW method, the choice of configurations σ in both methods, etc.

In what follows, we will examine these two issues in detail using a large number of fcc superstructures of the Pd-V system. Two methods will be used for direct calculations: The first-principles LDA approach and a tight-binding (TB) model thereof. Cluster expansions will then be performed using the CW and the DCA methods. In all cases, the energies will be given as excess, or formation quantities,

$$\Delta E(\sigma) = E(\sigma) - [(1-x)E(A) + xE(B)] \ , \qquad (13)$$

where x is the concentration of B atoms in the alloy. Thus, the formation energy gives an indication of the energy of σ relative to the phase separated pure elemental solids. The basic structure of our comparative tests is described in Fig. 1. We will assume that a computationally converged first-principles LDA calculation $E^{\rm LDA}_{\rm direct}(\sigma)$ [Eq. (1)] is "exact" for the present purpose,[45] and examine the extent to which various approaches mimic these quantities. LDA calculations will be executed within the method of linear muffin-tin orbitals within the atomic sphere approximation (LMTO-ASA),[46] and tested for a number of cases with respect to the more accurate full-potential linearized augmented plane wave[47] (LAPW) calculations. After a brief discussion of the extent to which LMTO-ASA mimics the more accurate LAPW method, we will compare the following (see Fig. 1):

(a) $\Delta E^{\rm LDA}_{\rm direct}(\sigma)$ vs $\Delta E^{\rm LDA}_{\rm CE-CW}(\sigma)$: ability of LDA-based Connolly-Williams cluster expansions [Eq. (5)] to predict [Eqs. (9), (10)] directly calculated LDA formation energies.

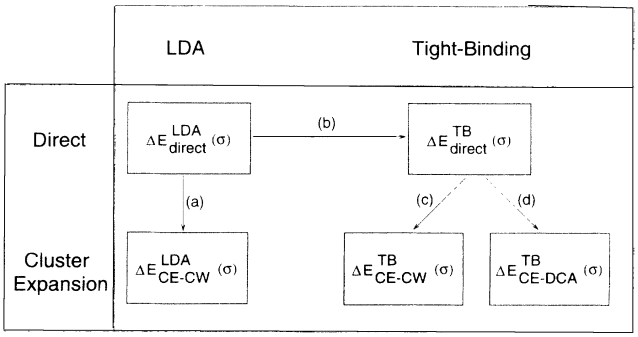

FIG. 1. Structure of the comparative tests of various direct calculations, and comparisons between direct and cluster expansion energies.

(b) $\Delta E^{\rm TB}_{\rm direct}(\sigma)$ vs $\Delta E^{\rm LDA}_{\rm direct}(\sigma)$: accuracy of direct tight-binding calculations with respect to direct LDA calculations of formation energies.

(c) $\Delta E^{\rm TB}_{\rm CE\text{-}CW}(\sigma)$ vs $\Delta E^{\rm TB}_{\rm direct}(\sigma)$: ability of TB-based Connolly-Williams cluster expansions [Eq. (5)] to predict [Eqs. (9), (10)] directly calculated TB formation energies.

(d) $\Delta E^{\rm TB}_{\rm CE\text{-}DCA}(\sigma)$ vs $\Delta E^{\rm TB}_{\rm direct}(\sigma)$: ability of TB-based DCA cluster expansions [Eq. (7)] to predict [Eqs. (9), (11)] directly calculated TB formation energies.

III. DETAILS OF CALCULATIONS

A. Direct LDA calculations: $\Delta E^{\rm LDA}_{\rm direct}$

Due to the relative ease and speed of the calculations, we have used here the LMTO-ASA method to calculate the total energy of a large number of Pd-V configurations. All structures considered are superstructures of the fcc lattice (i.e., the atoms of all unrelaxed configurations sit on the sites of an ideal fcc lattice). Most of the configurations Pd_nV_m may be grouped as "short-period" superlattices with periods $(n,m) \leq 5$ along several directions in direct space [(001), (111), (011), (201), (401), (311)]. Also included are several structures that are not superlattices, the most commonly occurring of these being the $L1_2$ (Cu_3Au) structure. There are several reasons why we select the Pd-V system for this study. (i) We have selected a "reactive system" for this study ($\Delta E \sim -250$ meV/atom at x=1/2) so that LDA and other errors will be *relatively* small. Atom pairs that are only slightly reactive (e.g., Cu-Pd, Cu-Au, Ni-Pt, with $|\Delta E| \lesssim 100$ meV/atom) are more difficult to treat precisely. (ii) The elemental solids, Pd and V, have a relatively small volume mismatch ($\Delta V/\overline{V} = 5.6\%$). Thus, our TB model, which completely neglects elastic energies, is applicable in principle. (iii) A cluster expansion with only pair terms will necessarily lead to formation energies that are completely symmetric about x=1/2. As shown below (and also elsewhere, see Ref. 4) the Pd-V system exhibits formation energies that are strongly asymmetric about x=1/2, thus implying that the cluster expansion

must contain significant multibody terms (terms corresponding to figures with three or more points). Thus, the Pd-V system provides a stringent test of the convergence of the cluster expansions.

The LMTO-ASA calculations were performed semirelativistically (including scalar relativistic corrections and excluding spin-orbit terms) with equal sphere radii for Pd and V. All structures were allowed to deform hydrostatically to their equilibrium volume, but cell-internal and cell-external relaxations were not considered. Two sets of LMTO-ASA calculations are discussed here. The structural energies of twenty compounds were computed by the present authors, for which the exchange-correlation potential of von Barth and Hedin used,[48] "combined corrections" (CC) terms to the ASA were included, and k point integration was performed with 4913 points in the full Brillouin zone, with the number of irreducible k points varying according to the symmetry of the structure considered. Additionally, the energies of twenty-three compounds are reported from Mikalopas,[49] for which the Hedin-Lundqvist exchange-correlation potential[50] was used, 245 irreducible k points were used and the CC terms were omitted.

Previous studies[42,49,51–56] have shown that in some specific cases, the LMTO-ASA method badly misrepresents the formation energies calculated within a full potential (e.g., LAPW) method. Some of these cases are collected in Table I. These large errors would render a CE based on these energies useless. Thus, to test our LMTO results for Pd-V, we compared them in a few cases to LAPW results. The LAPW calculations were performed with the Wigner exchange correlation[57] using muffin-tin radii of 2.4 a.u. for both Pd and V, and k-point integrations were carried out using 20–60 special points. The core (valence) electrons were treated fully (semi-) relativistically. The LAPW energies were minimized with respect to overall volume deformations as well as cell-internal and cell-external degrees of freedom. LMTO without CC gives formation energies[49] (with respect to fcc Pd and fcc V) of −292.4, −340.3,

TABLE I. Comparison of literature values of full-potential vs atomic sphere approximation (ASA) or muffin-tin (MT) formation energies of "problematic structures" showing large apparent ASA or MT errors. All energies are given in meV/atom. Values in parentheses designate fully relaxed energies.

Compound	Structure	Equivalent superlattice	ΔE Full potential	ΔE ASA/MT
NiV_3	$Z3$	$A_1B_3(001)$	-164.6(-164.6)[a]	-110.4[b]
NiV	$Z2$	$A_2B_2(001)$	-272.1(-292.1)[a]	-90.1[b]
Ni_3V	$Z1$	$A_3B_1(001)$	-214.7(-219.9)[a]	-129.1[b]
NiPt	$L1_0$	$A_1B_1(001)$	-77.7(-95.7)[c]	-28.6[d],-110.2[e], (-116.3)[f]
NiPt	$Z2$	$A_2B_2(001)$	(+3.2)[c]	-5.4(-53.0)[f]
NiPt	$L1_1$	$A_1B_1(111)$	(-29.5)[c]	-77.5(-80.2)[f]
AuPt	$B2$	$A_1B_1(001)$	(+132.1)[c]	(-43)[g] , (+66.7)[h]
Au_3Pt	$L1_2$		(+41.5)[c]	(-22)[g] , (+36.4)[h]
PtTi	$B2$	$A_1B_1(001)$	(-770)[i]	(-920)[j]
AuCs	$B2$	$A_1B_1(001)$	(~ -100)[k]	($\sim +400$)[l]

[a]Reference 42: LAPW with Wigner exchange correlation, lattice parameter from Vegard's law of calculated pure elements, and scalar-relativistic terms included.

[b]Reference 49: LMTO-ASA with Hedin-Lundqvist exchange correlation, calculated lattice constant, scalar-relativistic terms, equivolume atomic spheres, 245 k points, and "combined correction" terms omitted.

[c]Reference 51: LAPW with Wigner exchange correlation, lattice parameter from Vegard's law of calculated pure elements, scalar-relativistic terms included, and 60 special k points.

[d]Reference 52: LMTO-ASA with von Barth and Hedin exchange correlation, calculated lattice parameter, scalar-relativistic terms included, equivolume atomic spheres, 120 irreducible k points, and "combined corrections" included.

[e]Reference 52: LMTO-ASA with von Barth and Hedin exchange correlation, calculated lattice parameter, scalar-relativistic terms included, unequal sphere radii obtained from charge neutrality, 120 irreducible k points, and "combined corrections" included.

[f]Reference 53: LMTO-ASA with von Barth and Hedin exchange correlation, calculated lattice parameter, scalar-relativistic terms included, unequal sphere radii obtained by energy minimization, 120 k points, and "combined correction" terms included.

[g]Reference 54: Linearized atomic Slater-type orbital method (LASTO) (muffin-tin potential) with experimental lattice constant and scalar relativistic terms included.

[h]Present work: LMTO-ASA with von Barth and Hedin exchange correlation, calculated lattice parameter, scalar-relativistic terms included, equivolume atomic spheres, 165 irreducible k points, and "combined correction" terms included.

[i]Reference 55: LASTO (full potential) with experimental lattice constant of the low-temperature ($B19$) phase, and calculation performed fully relativistically.

[j]Reference 55: LASTO (muffin-tin potential) with experimental lattice constant of the low-temperature ($B19$) phase, and scalar-relativistic terms included.

[k]Reference 56: LASTO (full potential) with experimental lattice constant, 84 k points, and calculation performed fully relativistically.

[l]Reference 56: LASTO (muffin-tin potential) with experimental lattice constant, 84 k points, and calculation performed fully relativistically.

TABLE II. Pd-V structural energies for fcc superstructures. Direct LDA energies are from LMTO-ASA calculations described in the text. All energies in meV/atom. Designations in quotation marks indicate an alternate labeling scheme for structures for which no standard Strukturbericht exists.

Structure		Direct		Cluster expansion		
Superlattice	Designation	$\Delta E^{\mathrm{LDA}}_{\mathrm{direct}}$	$\Delta E^{\mathrm{TB}}_{\mathrm{direct}}$	$\Delta E^{\mathrm{TB}}_{\mathrm{CE\text{-}DCA}}$	$\Delta E^{\mathrm{TB}}_{\mathrm{CE\text{-}CWM}}$	$\Delta E^{\mathrm{LDA}}_{\mathrm{CE\text{-}CWM}}$
A (Pd)	fcc	0.0	0.0	0.0	0.0[a]	0.0[a]
B (V)	fcc	0.0	0.0	0.0	0.0[a]	0.0[a]
(001) Struct:						
A_1B_1	$L1_0$	-366.6(-353.8[b])	-539	-517	-521[a]	-358.1[a]
A_2B_2	"$Z2$"	-314.8(-292.4[b])	-355	-276	-362	-307.1[a]
A_3B_1	"$Z1$"	-225.9[b]	-258(-278[c])	-274	-284	-235.1[a]
A_1B_3	"$Z3$"	-229.5[b]	-310(-371[c])	-260	-339	-238.7[a]
A_2B_1	"$\beta 1$"		-354	-366	-378[a]	-317.6
A_1B_2	"$\beta 2$"		-437	-346	-453[a]	-322.4
(111) Struct:						
A_1B_1	$L1_1$	-241.3	-394	-289	-404[a]	-246.0[a]
A_2B_2	"$V2$"		-287	-185	-263[a]	-184.8
A_3B_1	"$V1$"		-213(-209[c])	-168	-204	-154.6
A_1B_3	"$V3$"		-260(-262[c])	-162	-262	-144.0
A_2B_1	"$\alpha 1$"		-265	-224	-271	-209.1
A_1B_2	"$\alpha 2$"		-336	-216	-350[a]	-195.1
(011) Struct:						
A_2B_2	"$Y2$"		-430	-338	-414[a]	-265.9
A_3B_1	"$Y1$"		-393(-322[c])	-343	-335	-253.9
A_1B_3	"$Y3$"		-356(-349[c])	-253	-340	-178.8
A_2B_1	$MoPt_2$ type	-393.5(-368.0[b])	-471	-469	-466	-359.5[a]
A_1B_2	$MoPt_2$ type	-181.1(-182.8[b])	-377	-287	-373[a]	-174.9[a]
A_5B_1	"$Y5$"	-191.5[b]		-234	-225	-177.0
A_1B_5	"$Y5_b$"	-123.1[b]		-167	-229	-116.6
A_4B_2	"$Y4$"	-185.6[b]		-235	-272	-189.9
A_2B_4	"$Y4_b$"	-174.4[b]		-244	-324	-201.2
A_3B_3	"$Y6$"	-218.3[b]		-251	-316	-208.8
$A_1B_1A_1B_3$	"$Y7$"	-240.8[b]		-399	-400	-286.0
$A_1B_1A_3B_1$	"$Y7_b$"	-293.0[b]		-346	-402	-246.3
$A_2B_1A_1B_2$	"$Y8$"	-270.4[b]		-389	-437	-284.5[a]
(201) Struct:						
A_2B_2	CH, or "40"	-243.7(-245.7[b])	-524	-473	-519	-260.1[a]
A_3B_1	$D0_{22}$	-348.4(-340.3[b])	-355(-377[c])	-439	-366[a]	-342.5[a]
A_1B_3	$D0_{22}$	-202.7(-208.3[b])	-311(-312[c])	-273	-320	-188.6[a]
A_4B_1	$D1_a$ (Ni_4Mo)	-269.6	-309	-352	-316	-302.4[a]
A_1B_4	$D1_a$ (Ni_4Mo)	-160.0	-237	-196	-261[a]	-168.7
(401) Struct:						
$A_5B_1A_1B_1$	$D0_{23}$		-357	-431	-343	-313.4
$A_1B_5A_1B_1$	$D0_{23}$		-345	-307	-344	-205.6
(311) Struct:						
A_2B_2	"$W2$"		-493	-409	-472	-318.1
A_3B_1	"$W1$"		-358(-316[c])	-320	-356	-257.4
A_1B_3	"$W3$"		-322(-304[c])	-225	-318	-203.4
Other Struct:						
A_3B_1	$L1_2$	-281.6(-281.7[b])	-319	-422	-320[a]	-284.3[a]
A_1B_3	$L1_2$	-204.6(-208.2[b])	-367	-341	-368[a]	-222.5[a]
A_8B_1	Ni_8Nb type	-195.6	-157(-157[c])	-195	-170	-169.6[a]
A_1B_8	Ni_8Nb type	-101.1	-160	-124	-173	-116.6
A_5B_1	'$W8$'	-240.7	-236	-292	-239	-228.6
A_1B_5	'$W8$'	-149.9	-241	-205	-256	-158.0
A_5B_3	'$W1$'	-341.8(-334.8[b])	-420	-478	-438	-349.8
A_3B_5	'$W1$'	-302.8(-302.3[b])	-407	-412	-452	-296.8[a]
Random:						
$A_{0.5}B_{0.5}$			-432	-352	-417	-265.8
$A_{0.75}B_{0.25}$			-272	-293	-308	-232.3
A_3B_1	$\Delta E(L1_2$ - $D0_{22})$	+66.8(+58.6[b])	+36(+58[c])	+17	+46	+58.2
A_1B_1	$\Delta E(L1_0$ - "40")	-122.9(-108.1[b])	-15	-43	-2	-98.0
Deviation (χ)		—	111.8[d]	64.8[e]	18.9[e]	18.8[d]

[a]Structure used in fit.
[b]LMTO-ASA without "combined corrections" (Ref. 49).
[c]TB model with "symmetry-distinct" charge neutrality (present work).
[d]Standard deviation with respect to LMTO.
[e]Standard deviation with respect to TB model.

and −281.7 meV/atom for the $Z2$, $D0_{22}$ (Pd_3V), and $L1_2$ (Pd_3V) structures, respectively. We find these three "LMTO with CC" [LAPW (Ref. 58)] energies to be −314.8 (−322.5), −348.4 (−350.2), and −281.6 (−278.6) meV/atom. The comparison between LAPW and LMTO is quite favorable in the case of Pd-V structures, especially when the CC are included.[59] The results of our LMTO calculations, $\Delta E^{\rm LDA}_{\rm direct}$ for 30 structures considered here are shown in the third column of Table II.

B. Direct TB calculations: $\Delta E^{\rm TB}_{\rm direct}$

There is a rich history of tight-binding calculations of properties of transition metals and their alloys: The strong bonding of the valence d electrons has been invoked to explain the cohesive[60] as well as structural[61] properties of the transition metals. These localized d electrons may be well described by the TB approximation, and therefore, many early calculations of formation energies in transition-metal *alloys*[62–64] were based on TB d-band-only models.

For the direct TB calculations of the present work, the formation energy of configuration σ is given by the relative "band energy" terms

$$\begin{aligned}\Delta E^{\rm TB}_{\rm direct}(\sigma) = &\int_{-\infty}^{E_F(\sigma)} E\, n(\sigma;E)dE \\ &- (1-x)\int_{-\infty}^{E_F(A)} E\, n(A;E)dE \\ &- x\int_{-\infty}^{E_F(B)} E\, n(B;E)dE \\ &- \frac{1}{N}\sum_i N_i\delta_i, \end{aligned} \tag{14}$$

neglecting explicit interelectronic Coulomb, exchange, and correlation corrections. Here $E_F(\sigma)$ is the Fermi level of σ, N_i is the locally neutral number of valence electrons on the atom at site i, δ_i is the potential shift of atom i (to be described below), and $n(\sigma;E)$ is the total density of states for σ, defined in terms of the eigenvalues of the alloy Hamiltonian:

$$H^{\rm TB}_{\rm alloy} = \sum_{i,\lambda} |i,\lambda\rangle \epsilon_i^\lambda \langle i,\lambda| + \sum_{j,k,\mu,\nu}^{j\neq k} |j,\mu\rangle \beta_{jk}^{\mu\nu} \langle k,\nu|. \tag{15}$$

The Latin indices designate lattice sites and the Greek indices label the orbitals. A nine orbital/atom (s+3p+5d) basis is used. The symbols ϵ_i^λ and $\beta_{jk}^{\mu\nu}$ denote the on-site energies and hopping integrals, respectively. Calculation of $\Delta E^{\rm TB}_{\rm direct}$ then requires as input the on-site energies for both A and B atoms, as well as hopping integrals (up to some small number of neighboring shells) between A-A, A-B, and B-B pairs of atoms. The Slater-Koster hopping integrals $\beta_{jk}^{\mu\nu}$ for first-nearest and second-nearest neighbor shells between like pairs A-A and B-B of atoms are given by TB-LMTO (Ref. 65) of the pertinent pure elements. The hopping between A-B pairs in the alloy is approximated by the geometric mean of the A-A and B-B integrals of the *pure solids*. The on-site energies ϵ_i^λ are those of the pure elements, with the A- and B-atom values shifted relative to one another by orbital-independent amounts, δ_i. These shifts δ_i along with the Fermi energy $E_F(\sigma)$ are determined by requiring each of the atoms of the alloy to be locally neutral

$$\int_{-\infty}^{E_F(\sigma)} n_i(\sigma;E)\,dE = N_i \quad \forall i, \tag{16}$$

where $n_i(\sigma;E)$ is the partial density of states on atom i in σ. For many structures, (e.g., $L1_0$, $L1_1$, $L1_2$, $MoPt_2$ type, etc.) the symmetry is such that all A atoms are symmetrically equivalent to all other A atoms, and similarly for B. For these types of structures, the assumption of local neutrality may be exactly satisfied by shifting only the on-site energies of all B atoms relative to their pure-element values by a single δ. However, many of the structures considered here (e.g., $D0_{23}$, Ni_8Nb type, *all* A_3B_1 superlattices, etc.) have symmetrically distinct, chemically identical atoms. In these cases, the shifts δ_i depend on the symmetry type of the atoms. This approach is called here the "symmetry-distinct neutrality condition". In contrast, there is an "average neutrality condition" whereby all chemically similar atoms have the same on-site potentials, and local neutrality is satisfied only in an average way. Note that the imposition of either neutrality condition introduces a dependence of both ϵ_i^λ and $\beta_{jk}^{\mu\nu}$ on the topology of the local environment, thus on the configuration σ.

All direct TB calculations were performed in both the "symmetry-distinct" and "average" charge neutrality approaches by decorating a ~1000-atom cluster with the appropriate (ordered or disordered) configuration, and then performing recursion[66] to obtain the densities of states, $n(\sigma;E)$, and hence the band energies of Eq. (14). Ten levels of recursion were used along with a quadratic terminator for the continued fraction.

It should be noted that the TB-LMTO calculations were performed at a single volume $\overline{V}$ given by the arithmetic average between calculated (as per LMTO) Pd and V pure element volumes. Thus, all terms of Eq. (14) are evaluated at $\overline{V}$ so these calculations do not take into account any form of atomic relaxation, and also do not account for energy lowerings from hydrostatic volume changes. The TB formation energies of Eq. (14) are thus with respect to the pure element energies at the *alloy* volume, rather than the *equilibrium* volume of the elemental solids, and will consequently lead to formation energies that are too negative. The correction between Eq. (14) [each term evaluated at constant $\overline{V}$] and Eq. (13) [each term evaluated at the equilibrium volume] is

$$\begin{aligned}\Delta E(\sigma) = \Delta E_{\rm TB}(\overline{V}) + \{&(1-x)[E_A(\overline{V}) - E_A(V_A)] \\ &+ x[E_B(\overline{V}) - E_B(V_B)]\}. \end{aligned} \tag{17}$$

The correction terms ("volume deformation") in curly brackets represent the energy change of the pure elements in deforming them hydrostatically from the alloy volume $\overline{V}$ to their respective equilibrium volumes, V_A and V_B. We have calculated this correction term via the LMTO-ASA, and we find that it assumes a maximum value of +19.6 meV/atom at $x = 1/2$. In comparing the TB energies with those of the LDA (for which all configurations are considered at their equilibrium volumes), we

should keep in mind that the TB values are *overbound* by roughly 20 meV/atom due to volume deformation effects.

The direct TB results, $E^{\rm TB}_{\rm direct}(\sigma)$, for σ = ordered, periodic configurations are shown in the fourth column of Table II. The two charge neutrality approaches yield similar formation energies (with differences $\lesssim 20$ meV/atom), except for the structures "$Z3$," "$Y1$," and "$W1$," where the differences are of the order of 50 meV/atom. In addition, the calculated $E^{\rm TB}_{\rm direct}$(random) for random alloys was performed via an average charge neutrality procedure by configurationally averaging over 50 randomly selected configurations of the ~1000-atom system. The DCA calculations to be described below use an average charge neutrality approach (with the potential shift as determined from the random equiatomic alloy), and hence it is this scheme of direct TB calculations which should be compared with the TB-cluster expansion results.

C. Cluster expansion—$\Delta E^{\rm LDA}_{\rm CE\text{-}CW}$ and $\Delta E^{\rm TB}_{\rm CE-CW}$

The methodology of the CW method relies on (a) the choice of figures and (b) the choice of configurations.

(a) *Figures*: We will use the same extended set of figures in the CW and DCA approaches. These are the "empty" figure [corresponding to a constant term in the cluster expansion of Eq. (3)], the "point" figure, the first- through fourth-nearest-neighbor pairs, four triplet figures, and four quadruplet figures. The vertices of these 14 figures are given in Table III as well as the degeneracies D_f. For the TB fit, is was found that including all four quadruplet interactions did not significantly improve the quality of the fit.

TABLE III. Vertices and degeneracies of fcc figures used in the CW and DCA-based cluster expansions.

Figure f	Degeneracy D_f	Site positions (in units of a=2)
Empty		
J_0	1	—
Point		
J_1	1	(0,0,0)
Pairs		
J_2	6	(0,0,0),(1,1,0)
K_2	3	(0,0,0),(2,0,0)
L_2	12	(0,0,0),(2,1,1)
M_2	6	(0,0,0),(2,2,0)
Triplets		
J_3	8	(0,0,0),(1,1,0),(1,0,1)
K_3	12	(0,0,0),(1,1,0),(2,0,0)
L_3	24	(0,0,0),(1,1,0),(2,1,1)
Q_3	6	(0,0,0),(1,1,0),(2,2,0)
Quadruplets		
J_4	2	(0,0,0),(1,1,0),(1,0,1),(0,1,1)
K_4	12	(0,0,0),(1,1,0),(1,0,1),(2,0,0)
M_4	6	(0,0,0),(1,1,0),(2,2,0),(3,3,0)
SQ	3	(0,0,0),(1,1,0),(-1,1,0),(0,2,0)

(b) *Configurations*: A large number (~500 000) of different sets of configurations were tried, with the final selection being determined by the input set whose predictive error [i.e., the difference between predicted and directly calculated energies, the root-mean-square of Eq. (12)] was a minimum. It was found that an input set of 18 configurations provided for a small fitting error, and still left many structures to test the predictive ability of the fit. These configurations used as input to the cluster expansion are denoted in Table II with a superscript "a."

The calculation of $\Delta E^{\rm LDA}_{\rm CE\text{-}CW}$ used $\{\Delta E^{\rm LDA}_{\rm direct}(\sigma)\}$ as computed by LMTO as input, and values with "combined corrections" are preferred when two LMTO values are available. For the calculations of $\Delta E^{\rm TB}_{\rm CE\text{-}CW}$, we used as input the $\{\Delta E^{\rm TB}_{\rm direct}(\sigma)\}$ values as computed from the average charge neutrality approach. The results of $\Delta E^{\rm LDA}_{\rm CE\text{-}CW}$ and $\Delta E^{\rm TB}_{\rm CE\text{-}CW}$ are given in columns 6 and 7 in Table II.

Additionally, tests were performed (for the LDA energies) to assess the stability of the fit with respect to the 14 figures and 18 configurations. It was found that the predictive error was relatively insensitive to the particular choice of configurations, as roughly 10% (~50 000) of the configuration sets tried had predictive errors that were less than 20 meV/atom. (The minimum and maximum predictive errors found were 18.8 and 37.7 meV/atom, respectively.) The fits were also found to be stable with respect to changes in one or two of the figures included. For instance, if only 13 figures are included by eliminating the square figure (Table III), the minimum predictive error is only marginally increased from 18.8 to 19.2 meV/atom, and further eliminating M_4 from the fit and using only 12 figures provides a predictive error of 19.3 meV/atom. However, if a significant interaction (a figure that gives a sizeable contribution to the expansion) is eliminated from the fitting procedure, the fit becomes more unstable, and the predictive error rises sharply (e.g., using 13 figures, with J_3 eliminated, the predictive error increases from 18.8 to 25.2 meV/atom). Such tests determine which figures are "important" and should not be omitted.

In Ref. 49, Mikapolas *et al.* tested the convergence and stability of the CW procedure using the energies of a large number of Ni-V and Pd-V alloys, as calculated from the LMTO. The CW fits were performed for a variety of sets of figures and configurations, however, of the figures used in Ref. 49, only two (pair) figures extend beyond the fcc *second*-nearest-neighbor distance. In contrast, the figures used in this study (Table III) include pair, triplet, and quadruplet figures, all of which extend to (or beyond) the fcc *fourth*-nearest-neighbor distance. Also, in all of the fits of Mikapolas *et al.*, the number of structures used was equal to the number of figures kept in the expansion, thus, the direct inversion of Eq. (6) is used, rather than the over-determined optimization of Eq. (5) which is used here. Mikapolas *et al.*[49] failed to find a stable CE (i.e., the fits were quite sensitive to the particular choice of configurations and figures used), in contrast to the stable results presented here. We, therefore, conclude

that the sensitivity of the fits of Mikapolas *et al.* were due to (1) the small number of long-ranged figures used in the expansion and (2) the use of a direct inversion of Eq. (6), rather than the singular value decomposition of Eq. (5).

D. Cluster expansion—$\Delta E^{\rm TB}_{\rm CE\text{-}DCA}$

The DCA calculations for Pd-V have been described in depth previously.[4] Here, we merely give the salient details. The interaction energies are obtained via Eq. (7), using the recursion method, along with the formalism of "orbital peeling"[67] to avoid numerical instabilities associated with taking the small differences of large numbers inherent in Eq. (7). Averages were taken over 50 configurations for the pair figures, 15–30 for triplets, and 10–20 for quadruplets. The convergence of configurational averages with increasing size of the figure is discussed in the Appendix of Ref. 4. The same specifics of the recursion method used in the direct TB calculations discussed above were also used in the DCA computations. System sizes of $\gtrsim 1000$ atoms were used in the DCA calculation of the interactions, with the precise number of atoms corresponding to five complete shells of first-nearest and second-nearest-neighbors surrounding the two-, three-, or four-point figure. The results of $\Delta E^{\rm TB}_{\rm CE\text{-}DCA}$ are given in column 5 of Table II.

IV. RESULTS

The main results of this paper are given in Table II. In this table, we compare the formation energies for Pd-V alloys as computed from all of the methods described above. A graphical representation of this data is also given in Fig. 2. Our discussion (Sec. IV A–IV D) will follow, respectively, the four steps (a)–(d) described in Sec. II and Fig. 1. We will characterize each step by the rms error χ between the two sets of energies. In assessing these errors χ, we should bear in mind the typical median formation energy [Fig. 2(a)] in this reactive system: -250 meV/atom.

A. $\Delta E^{\rm LDA}_{\rm direct}$ vs $\Delta E^{\rm LDA}_{\rm CE\text{-}CW}$

Here we describe the ability of the LDA-based Connolly-Williams cluster expansion of Eq. (6) to predict [Eqs. (9), (10)] directly calculated LDA energies. The direct LDA (LMTO) calculations and the CW fit to these values are shown in the third and seventh columns of Table II, and are plotted in Fig. 2(a). The quality of the fit is good and leads to a standard deviation between calculated and fitted energies of $\chi = 18.8$ meV/atom (of the same order as the difference between the two underlying LMTO calculations described in Table II). Even the predicted energies of structures not used in the fit [see, e.g., many of the (011) superlattices] are reasonably close to the directly calculated values. And, the structural en-

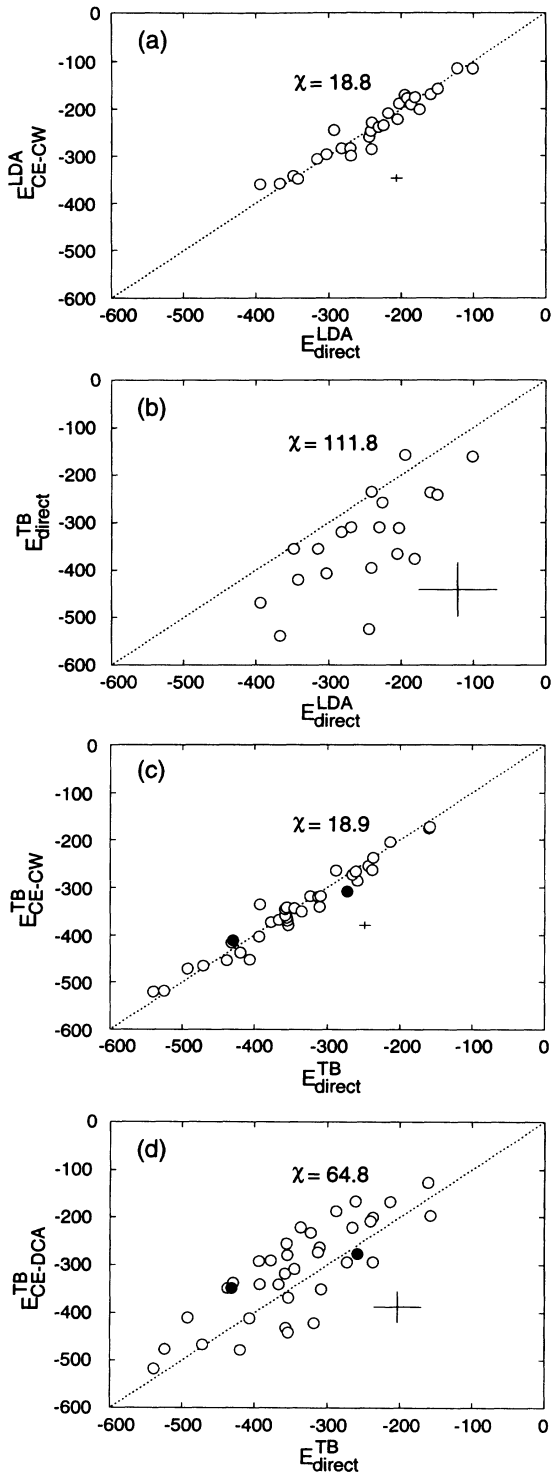

FIG. 2. Pictorial representation of Pd-V formation energies (in meV/atom) of Table II. Comparisons are shown for: (a) $E^{\rm LDA}_{\rm direct}$ vs $E^{\rm LDA}_{\rm CE\text{-}CW}$, (b) $E^{\rm LDA}_{\rm direct}$ vs $E^{\rm TB}_{\rm direct}$, (c) $E^{\rm TB}_{\rm direct}$ vs $E^{\rm TB}_{\rm CE\text{-}CW}$, and (d) $E^{\rm TB}_{\rm direct}$ vs $E^{\rm TB}_{\rm CE\text{-}DCA}$. Each ordered structure is represented by an open circle, and in parts (c) and (d), random alloys of compositions x=1/2 and x=1/4 are denoted by filled circles. The dotted diagonal lines indicate points of exact agreement between various sets of formation energies, and the crosses denote the size of the standard deviation (χ) between the various sets. In parts (a) and (b), $E^{\rm LDA}_{\rm direct}$ refers to LMTO calculations.

ergy differences between two competing configurations at the same composition (e.g., $L1_2 - D0_{22}$ or $L1_0$ – "40") are adequately represented by the fit. The predictive errors of the fits should be considered in light of the errors inherent in the direct LDA calculations, which are $\sim$ 10 meV/atom or less.

B. $\Delta E^{\rm TB}_{\rm direct}$ vs $\Delta E^{\rm LDA}_{\rm direct}$

Here we assess the ability of the TB model [Sec. III B] to mimic the directly calculated LDA formation energies. The comparison between direct LDA vs TB calculations shown in the third and fourth columns of Table II and in Fig. 2(b) shows immediately that the TB model tends to predict a significant and systematic overbinding (formation energies that are significantly too negative), as compared to the LDA. The discrepancy between the TB calculations and LDA ranges all the way from 5 meV/atom for '$W8$' (Pd_5V) to 280 meV/atom for the CH ("40") structure.[68] The average deviation between the LDA and TB calculations is χ = 111.8 meV/atom.[69] In some instances the discrepancies are large enough to alter the ground state symmetry and/or structure type predicted within a family of structures. For example: (a) within the (201) family, LDA predicts structure $D0_{22}$ to have the lowest energy within this group, while TB predicts the "40" to be the lowest. (b) The LDA predicts Pd_3V to be more stable than PdV_3 in the $L1_2$ structure, and TB gives the reverse order of stability. (c) The LDA predicts Pd_8V to be more stable than PdV_8 in the Ni_8Nb-type structure and the TB predicts the reverse. The same is true for Pd_5V and PdV_5 in the '$W8$' structure. (d) The LDA predicts a large difference between $L1_0$ (−354 meV/atom) and "40" (−246 meV/atom) formation energies, suggestive of the existence of long-range interactions (as these two structures are degenerate in energy for any nearest-neighbor-only cluster expansion), while the TB places these structures at similar energies (−539 meV/atom and −524 meV/atom, respectively).

The overbinding of the TB seems to be a general feature of this model. In Table IV, we present partial results analogous to those of Table II for several other transition-metal alloy systems. In the highly reactive Pd-Ti and Pt-V systems the TB calculation of the $L1_0$ structure yields −769 and −881 meV/atom, respectively, much more negative than the analogous LDA calculation of −583 and −589 meV/atom, respectively. The reason for this systematic overbinding is not understood at this time, but it appears to correlate with the reactivity of the system: In the nonreactive Pd-Rh system, the TB [$\Delta E^{\rm TB}_{\rm direct}(L1_0)$ = +93.9 meV/atom] and LDA [$\Delta E^{\rm LDA}_{\rm direct}(L1_0)$ = +94.2 meV/atom] $L1_0$ calculations are virtually identical. Hopefully, tight-binding practitioners could improve the accuracy of this scheme relative to direct LDA calculations.

Our preceding discussion referred to the correlation between LDA and TB *formation energies* of given configurations σ. A formation energy can be written also in terms of *cohesive energies* $E_c = E_{\rm solid} - E_{\rm atoms}$, i.e.,

TABLE IV. Formation energies for Pd-Rh, Pd-Ti, and Pt-V alloys. All energies are in meV/atom. Direct LDA energies are from LMTO-ASA calculations of the present work, described in the text ("combined correction" terms included). For the calculated Pd-Ti and Pt-V energies, the formation energies are taken with respect to the equilibrium structure of the pure elements (i.e., bcc V and hcp Ti) so that they may be adequately compared with experiment. To this end, all cluster expansion results (which are with respect to fcc pure elements) are supplemented by the relevant structural energy differences of the pure elements, as computed from LDA. Note that this is to be distinguished from the Pd-V energies of Table II, which are with respect to fcc pure elements.

Alloy		Direct		Cluster expansion		Experiment
System	Structure	$\Delta E^{\rm LDA}_{\rm direct}$	$\Delta E^{\rm TB}_{\rm direct}$	$\Delta E^{\rm TB}_{\rm CE\text{-}DCA}$	$\Delta E^{\rm TB}_{\rm CE\text{-}CW}$	$\Delta E_{\rm expt}$
Pd-Rh	$L1_0$	+94.2	+93.9	+99.7	+94.7	
	$Pd_{0.50}Rh_{0.50}$		+66.2	+71.7	+56.8	+104[a]
Deviation	χ		11.2	12.1	3.9	
Pd-Ti	$L1_0$	-583.1	-769	-478	-754	-550[b]
	$L1_2$ (Pd_3Ti)	-692.1	-562	-528	-553	-525[c]
	$Pd_{0.50}Ti_{0.50}$		-581	-308	-625	
Deviation	χ		195	299	21	
Pt-V	$L1_0$	-588.8	-881	-638	-841	-407[d]
	$Pt_{0.50}V_{0.50}$		-735	-324	-637	
Deviation	χ			218	34.5	

[a]Reference 70.

[b]Reference 71: The experimental measurement for $Pd_{0.50}Ti_{0.50}$ was on a combination of orthorhombic and cubic phases, and should provide a lower bound for the enthalpy of formation of the metastable $L1_0$ (tetragonal) phase.

[c]Reference 71.

[d]Reference 72: The experimental measurement for PtV is for the stable $B19$ phase, and should provide a lower bound for that of metastable $L1_0$.

$$\Delta E^{\rm TB}_{\rm direct}(\sigma) = E^{\rm TB}_c(\sigma) - [(1-x)E^{\rm TB}_c(A) + xE^{\rm TB}_c(B)], \quad (18a)$$

$$\Delta E^{\rm LDA}_{\rm direct}(\sigma) = E^{\rm LDA}_c(\sigma) - [(1-x)E^{\rm LDA}_c(A) + xE^{\rm LDA}_c(B)]. \quad (18b)$$

Thus, errors in the total energy of the *free atoms* (e.g., correlation errors) are exactly cancelled in $\Delta E_{\rm direct}$. The TB errors noted in Fig. 2(b) reflect the combination of errors in the cohesive energy of the *compound* σ and those of the *elemental solids* A and B.

If one is interested, however, only in $T = 0$ K *structural* energies $\delta\Delta E(\sigma,\sigma')$ rather than in formation energies and $T \neq 0$ phase diagrams, a different comparison suggests itself, namely

$$\delta\Delta E^{\rm TB}_{\rm direct}(\sigma,\sigma') = E^{\rm TB}_c(\sigma) - E^{\rm TB}_c(\sigma'), \quad (19a)$$

$$\delta\Delta E^{\rm LDA}_{\rm direct}(\sigma,\sigma') = E^{\rm LDA}_c(\sigma) - E^{\rm LDA}_c(\sigma'). \quad (19b)$$

Here σ and σ' are different configurations at the same composition. In contrast to the formation energies of Eq. (18a), the errors in the *elemental* cohesive energies cancel exactly. Table II shows for example that at $x = 3/4$, we have $\delta\Delta E^{\rm TB}_{\rm direct}(L1_2, D0_{22}) = +58$ (+36) meV/atom, using the "symmetry distinct (average) neutrality condition" while $\delta\Delta E^{\rm LDA}_{\rm direct}(L1_2, D0_{22}) = +67$ meV/atom. Similarly at $x = 1/2$, $\delta\Delta E^{\rm TB}_{\rm direct}(L1_0, \text{"40"}) = -15$ meV/atom, while $\delta\Delta E^{\rm LDA}_{\rm direct}(L1_0, \text{"40"}) = -123$ meV/atom, and $\delta\Delta E^{\rm TB}_{\rm direct}(L1_0, L1_1) = -145$ meV/atom, while $\delta\Delta E^{\rm LDA}_{\rm direct}(L1_0, L1_1) = -125$ meV/atom. Thus, the average deviation for *structural* energies in these cases is $\chi = 78$ meV/atom out of an average $|\delta\Delta E|$ of 105 meV/atom.

It is useful to distinguish alloy properties that are directly affected by errors in formation energies ("type I" properties, i.e., phase diagrams, transition temperatures) from alloy properties sensitive to errors in ratios of structural energies ("type II" properties). The preceding comparisons raise some interesting questions as to how the systematic overbinding of the TB energies might manifest itself in type I vs type II properties. Assume a model calculation scheme ($\Delta E^{\rm model}_{\rm direct}$) for which the overbinding relative to LDA is *uniform*, i.e.,

$$\Delta E^{\rm model}_{\rm direct}(\sigma) = \lambda \Delta E^{\rm LDA}_{\rm direct}(\sigma), \quad (20)$$

with λ a constant, independent of σ. The overbinding of the model system would then translate through Eqs. (6) and (7) into interaction parameters which are scaled by λ

$$J_f^{\rm model} = \lambda J_f^{\rm LDA}. \quad (21)$$

Hence, in $T \neq 0$ K composition-temperature phase diagrams (type I alloy properties), the uniform overbinding of Eq. (20) would propagate into transition temperatures of the model system which are overestimated with respect to LDA by a factor of λ: $T_c^{\rm model} = \lambda T_c^{\rm LDA}$. However, for a set of J_f, the ground state structures as a function of alloy composition are dependent not on the absolute magnitude of the J_f, but rather on their *ratios*.[2] From Eq. (21), the ratios of $J_f^{\rm model}$ are equal to the ratios of $J_f^{\rm LDA}$

$$\frac{J_1^{\rm model}}{J_2^{\rm model}} = \frac{J_1^{\rm LDA}}{J_2^{\rm LDA}}. \quad (22)$$

Thus, even in the presence of a uniform overbinding, the T=0 K ground state structures of the model system (type II properties) would be precisely those of the LDA. Our present calculations for the *chemically reactive* Pd-V system shows, unfortunately, that the overbinding in TB energies, while systematic, is not uniform, so both type I and type II alloy properties of the TB model need not necessarily be very accurate. However, it should be noted that the TB model used here has been shown to give an accurate depiction of the ground state structures[4] (type II) and site substitution behavior[73] (type II) for a variety of alloy systems, and also in the case of one *nonreactive* system (Pd-Rh), an accurate composition-temperature phase diagram[15] (type I).

C. $\Delta E^{\rm TB}_{\rm CE\text{-}CW}$ vs $\Delta E^{\rm TB}_{\rm direct}$

Here we assess the ability of the TB-based Connolly-Williams cluster expansion to predict the directly calculated TB formation energies. The direct TB calculations vs the CW fit to these numbers may be seen in Fig. 2(c) and by contrasting columns 4 and 5 of Table II. The standard deviation of this fit [$\chi = 18.9$ meV/atom) is almost equal to that of the LDA-based fit [18.8 meV/atom in Fig. 2(a)]. For Pd-Rh, Pd-Ti, and Pt-V, the standard deviations of the CW fits (Table IV), $\Delta E^{\rm TB}_{\rm direct}$ are $\chi =$ 3.9, 21.0, and 34.5 meV/atom, respectively. To assess the scale of these discrepancies, the reader must keep in mind that for PdRh, PdTi, and PtV, the values of $\Delta E^{\rm TB}_{\rm direct}(L1_0)$ are +93.9, −769, and −881 meV/atom, respectively. The ratio of the CW deviation and the directly calculated TB values of the $L1_0$ structure (which gives a scale for the reactivity of the system) are roughly equal for the four systems studied: $\chi/|\Delta E^{\rm TB}_{\rm direct}(L1_0)| =$ 0.035, 0.042, 0.027, and 0.039 for Pd-V, Pd-Rh, Pd-Ti, and Pt-V, respectively. These values are also close to that of the CW fit to the direct LDA energies for Pd-V: $\chi/|\Delta E^{\rm LDA}_{\rm direct}(L1_0)| = 0.051$. Thus, the Connolly-Williams cluster expansion is able to fit equally well either TB or direct LDA energies. However, while the quality of the fit appears to be equal, the accuracy of the energies entering the fit is the true limiting factor here (see Sec. IV B).

D. $\Delta E^{\rm TB}_{\rm CE\text{-}DCA}$ vs $\Delta E^{\rm TB}_{\rm direct}$

Here we assess the ability of the TB-based DCA cluster expansion to predict the directly calculated TB formation energies. The comparison between direct TB energies and those as calculated from the DCA is shown

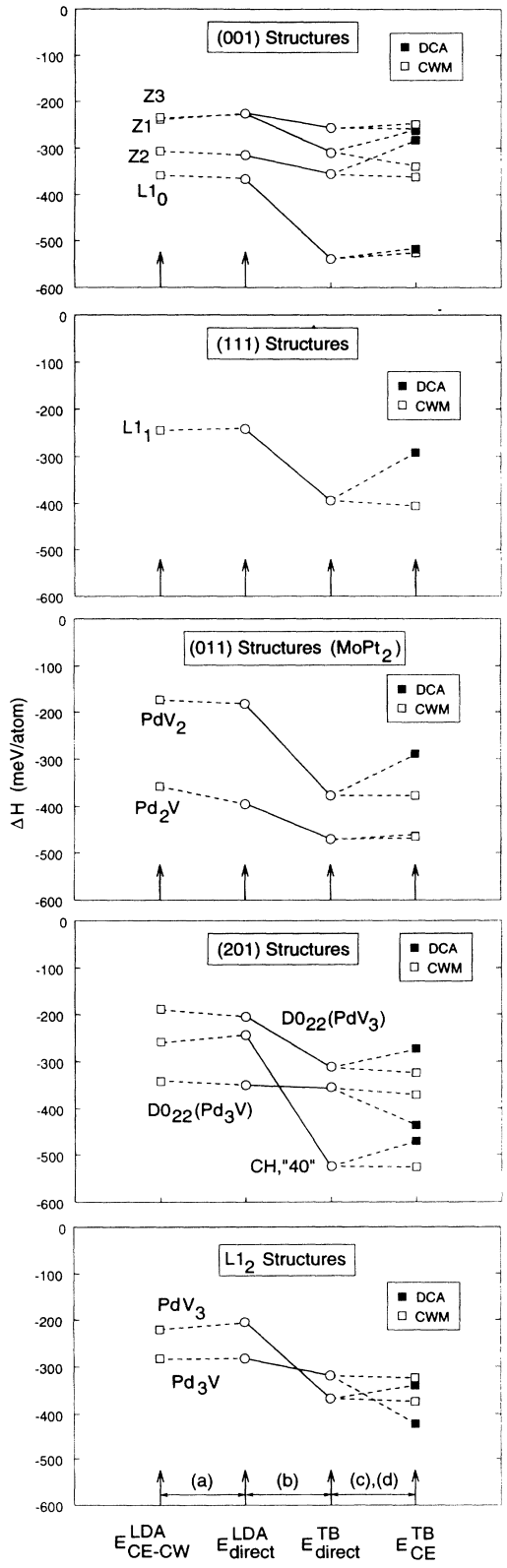

FIG. 3. Comparison of direct LDA and TB calculations (open circles connected by solid lines) with the corresponding cluster expansion values (open and filled squares, connected to direct calculations by dotted lines). The slopes of the lines in this figure indicate the errors between relative sets of energies.

in columns 4 and 5 of Table II, and in Fig. 2(d). The deviation between these two sets of numbers is 64.8 meV/atom, which is much larger than the CW fit to the TB calculations. A similar trend is observed in Table IV for Pd-Ti and Pt-V (the standard deviations of $\Delta E^{TB}_{CE\text{-}DCA}$ vs ΔE^{TB}_{direct} are 299 and 218 meV/atom, respectively), while for Pd-Rh we find that the DCA cluster expansion gives a relatively good fit to the formation energies (χ = 12.1 meV/atom), although the deviation is still larger than that of the corresponding CW fit. Interestingly, the DCA-cluster expansion values (using as input energies of random configurations) for the energies of *random* $Pd_{0.50}V_{0.50}$ and $Pd_{0.75}V_{0.25}$ alloys are no closer to the direct calculations than are the CW values (which use as input only the energies of *ordered* structures). For random $Pd_{0.50}Ti_{0.50}$ and $Pt_{0.50}V_{0.50}$ alloys, the trend is the same, as the DCA values (−308 and −324 meV/atom) do not compare as well to ΔE^{TB}_{direct}(random) (−581 and −735 meV/atom) as the CW fitted numbers (−625 and −637 meV/atom).

V. CONCLUSIONS

Many of the trends of the preceding section may be summarized in a graphical fashion in Fig. 3. In this figure, we plot the energies for many of the superlattice families given in Table II: The direct TB and LMTO calculation are shown as open circles, connected by solid lines, while the cluster expansion values are shown as open or filled squares, connected to the relevant direct calculation by dotted lines. Thus, from the slopes of the lines in Fig. 3, the general trends emerge: The direct TB calculations generally predict significant "overbinding" (i.e., formation energies that are too negative compared to the LMTO values). Thus, the TB formalism should be refined before it can systematically be used in quantitative calculations of structural stability in transition metals. The CW fits are generally good (the slopes of these dotted lines are nearly zero), and the DCA values do not compare as well to the direct TB energies. In general, the DCA energies tend to be significantly less negative than the direct TB computations, thus partially reversing the trend of the overbinding of the TB. This reversal must be somewhat fortuitous, though, as the DCA calculations should, at best, be able to reproduce the direct TB results.

ACKNOWLEDGMENTS

This work was supported by the Office of Energy Research (OER) [Division of Materials Science of the Office of Basic Energy Sciences (BES)], U. S. Department of Energy, under Contract No. DE-AC36-83 CH10093.

[1] F. Ducastelle, *Order and Phase Stability in Alloys* (Elsevier, New York, 1991).
[2] J. Kanamori and Y. Kakehashi, J. Phys. (Paris) Colloq. **38**, C7-274 (1977).
[3] Z.-W. Lu, S.-H. Wei, and A. Zunger, Phys. Rev. Lett. **66**, 1753 (1991).
[4] C. Wolverton, G. Ceder, D. de Fontaine, and H. Dreyssé, Phys. Rev. B **48**, 726 (1993).
[5] For a collection of articles, see *Alloy Phase Stability*, edited by G. M. Stocks and A. Gonis, NATO Advanced Study Institute Series (Kluwer, Dordrecht, 1989).
[6] For a collection of articles, see *Statics and Dynamics of Alloy Phase Transformations*, edited by P. E. A. Turchi and A. Gonis, NATO Advanced Study Institute Series (Plenum, New York, 1994).
[7] See, e.g., *Alloy Phase Stability and Design*, edited by G. M. Stocks, D. Pope, and A. Giamei, MRS Symposia Proceedings No. 186 (Materials Research Society, Pittsburgh, 1991).
[8] L. G. Ferreira, S. -H. Wei, and A. Zunger, Phys. Rev. B **40**, 3197 (1989).
[9] M. Sluiter, D. de Fontaine, X. Q. Guo, R. Poloucky, and A. J. Freeman, Phys. Rev. B **42**, 10 460 (1990).
[10] S.-H. Wei, L. G. Ferreira, and A. Zunger, Phys. Rev. B **41**, 8240 (1990).
[11] Z. -W. Lu, S. -H. Wei, A. Zunger, S. Frota-Pessoa, and L. G. Ferreira, Phys. Rev. B **44**, 512 (1991).
[12] J. M. Sanchez, J. P. Stark, and V. L. Moruzzi, Phys. Rev. B **44**, 5411 (1991).
[13] P. E. A. Turchi, M. Sluiter, F. J. Pinski, D. D. Johnson, D. M. Nicholson, G. M. Stocks, and J. B. Staunton, Phys. Rev. Lett. **67**, 1779 (1991).
[14] M. Asta, D. de Fontaine, and M. van Schilfgaarde, J. Mater. Res. **8**, 2554 (1993).
[15] C. Wolverton, D. de Fontaine, and H. Dreyssé, Phys. Rev. B **48**, 5766 (1993).
[16] W. Selke, Phys. Rep. **170**, 213 (1988).
[17] C. Cheng, R. J. Needs, V. Heine, and I. L. Jones, Phase Transitions **16/17**, 263 (1989).
[18] A. Qteish, V. Heine, and R. J. Needs, Physica B **185**, 366 (1993).
[19] R. G. Dandrea, J. E. Bernard, S. -H. Wei, and A. Zunger, Phys. Rev. Lett. **64**, 36 (1990).
[20] D. B. Laks, L. G. Ferreira, S. Froyen, and A. Zunger, Phys. Rev. B **46**, 12 587 (1992).
[21] U. Klemradt, B. Drittler, R. Zeller, and P. H. Dederichs, Phys. Rev. Lett. **64**, 2803 (1990).
[22] H. M. Petrilli and S. Frota-Pessoa, Phys. Rev. B **48**, 1748 (1993).
[23] J. E. Northrup and S. B. Zhang, Phys. Rev. B **47**, 6791 (1993).
[24] D. Vanderbilt and C. Y. Lee, Phys. Rev. B **45**, 11 192 (1992).
[25] W. R. L. Lambrecht, C. Amador, and B. Segall, Phys. Rev. Lett. **68**, 1363 (1992).
[26] T. Hong and A. J. Freeman, J. Mater. Res. **7**, 68 (1992).
[27] C. Woodward, J. M. MacLaren, and S. Rao, J. Mater. Res. **7**, 1735 (1992).
[28] M. C. Payne, M. P. Teter, D. C. Allan, T. A. Arias, and J. D. Joannopoulos, Rev. Mod. Phys. **64**, 1045 (1992).
[29] G. Galli and M. Parrinello, Phys. Rev. Lett. **69**, 3547 (1992).
[30] X. -P. Li, R. W. Nunes, and D. Vanderbilt, Phys. Rev. B **47**, 10 891 (1993).
[31] S. Baroni and P. Giannozzi, Europhys. Lett. **17**, 547 (1992).
[32] F. Mauri, G. Galli, and R. Car, Phys. Rev. Lett. **47**, 9973 (1993).
[33] A review is given by A. Zunger, in *Statics and Dynamics of Alloy Phase Transformations* (Ref. 6).
[34] D. de Fontaine, Solid State Phys. (to be published).
[35] J. M. Sanchez, F. Ducastelle, and D. Gratias, Physica A **128**, 334 (1984).
[36] M. Asta, C. Wolverton, D. de Fontaine, and H. Dreyssé, Phys. Rev. B **44**, 4907 (1991).
[37] J. M. Sanchez, Phys. Rev. B **48**, 14 013 (1993).
[38] J. W. D. Connolly and A. R. Williams, Phys. Rev. B **27**, 5169 (1983).
[39] H. Dreyssé, A. Berera, L. T. Wille, and D. de Fontaine, Phys. Rev. B **39**, 2442 (1989).
[40] C. Wolverton, A. Zunger, and Z. -W. Lu, Phys. Rev. B, **49**, 16 058 (1994).
[41] Z. -W. Lu and A. Zunger, Phys. Rev. B **50**, 6626 (1994).
[42] Z. -W. Lu, D. B. Laks, S. -H. Wei, and A. Zunger, Phys. Rev. B **50**, 6642 (1994).
[43] The summation in Eq. (10) is only over the N_F symmetry-distinct figures, however, that of Eq. (11) includes these N_F figures and all symmetry-related sets of lattice points. Hence, the "lattice-averaged products" are explicitly included in Eq. (10), but not in Eq. (11).
[44] For the case of $N_\sigma = N_F$, the configurations used in Eq. (6) must by chosen so that the matrix, $\widetilde{\Pi}$, is nonsingular. However, there are many sets of configurations that lead to a nonsingular $\widetilde{\Pi}$ and hence Ferreira *et al.* (Ref. 8) have proposed a criterion for choosing a set of input structures, tailored to insure a proper convergence of the energy of the random alloy. In the overdetermined case of Eq. (5), a criterion has also been put forth (Ref. 14) which amounts to choosing the set of configurations so as to give the "most orthogonal" values of $\widetilde{\Pi}_f(\sigma)$.
[45] Each of the three terms in the definition of the formation energy [Eq. (13)] may be considered as the cohesive energy, i.e., the total energy of the solid minus the energy of an equivalent number of isolated *atoms*. It is well known that the LDA gives a systematic overbinding for the cohesive energies of solids. Much of this overbinding results from a rather poor description of the energies of free atoms. However, these free atom terms cancel *exactly* when considering the *formation* energy of Eq. (13). It is thus likely that when considering formation energies of alloy systems, errors induced by the LDA are much smaller than those of the cohesive energies.
[46] O. K. Andersen, Phys. Rev. B **12**, 3060 (1975).
[47] S. -H. Wei and H. Krakauer, Phys. Rev. Lett. **55**, 1200 (1985), and references cited therein.
[48] U. von Barth and L. Hedin, J. Phys. C **5**, 1629 (1972).
[49] J. Mikalopas, Ph.D. thesis, University of California at Davis, 1993; J. Mikalopas, P. Sterne, P. Turchi, M. Sluiter and A. Gonis (unpublished).
[50] L. Hedin and B. I. Lundqvist, J. Phys. C **4**, 2064 (1971).
[51] Z. -W. Lu, S. -H. Wei, and A. Zunger, Europhys. Lett. **21**, 221 (1993).
[52] P. P. Singh and A. Gonis, Phys. Rev. B **49**, 1642 (1994).
[53] C. Amador, W. R. L. Lambrecht, and B. Segall, in *Application of Multiple Scattering Theory to Materials Science*, edited by W. H. Butler, P. H. Dederichs, A. Gonis, and R. Weaver, MRS Symposia Proceedings No. 253 (Material Research Society, Pittsburgh, 1992), p. 297.

[54] R. E. Watson, J. W. Davenport, and M. Weinert, Phys. Rev. B **35**, 508 (1987).
[55] G. W. Fernando, R. E. Watson, and M. Weinert, Phys. Rev. B **45**, 8233 (1992).
[56] R. E. Watson and M. Weinert, Phys. Rev. B **49**, 7148 (1994).
[57] E. Wigner, Phys. Rev. **46**, 1002 (1934).
[58] Z. -W. Lu (private communication).
[59] Errors due to the ASA may be divided into those resulting from the overlap of the atomic spheres, and also from the assumption of spherical symmetry of potential and charge density. Because the CC is an approximate attempt to treat the former types of errors, but not the latter, the agreement with LAPW indicates that the shape approximations inherent in the ASA introduce negligible errors for Pd-V alloys.
[60] J. Friedel, in *The Physics of Metals*, edited by J. M. Ziman (Cambridge University Press, London, 1969), Chap. 8.
[61] F. Ducastelle and F. Cyrot-Lackmann, J. Phys. Chem. Solids **31**, 1295 (1970); **32**, 285 (1971).
[62] J. van der Rest, F. Gautier, and F. Brouers, J. Phys. F **5**, 2283 (1975).
[63] M. Cyrot and F. Cyrot-Lackmann, J. Phys. F **6**, 2257 (1976).
[64] D. G. Pettifor, Phys. Rev. Lett. **42**, 846 (1979).
[65] O. K. Andersen and O. Jepsen, Phys. Rev. Lett. **53**, 2571 (1984).
[66] R. Haydock, Solid State Phys. **35**, 215 (1980).
[67] N. R. Burke, Surf. Sci. **58**, 349 (1976).
[68] The Ni_8Nb (Pd_8V) and "$W8$" (Pd_5V) structures and the only ones for which the LDA formation energies are more negative than the TB.
[69] One should keep in mind the effect of energy lowerings from hydrostatically deforming the elemental solids, Pd and V. If included, this effect would account for TB formation energies which—at $x=1/2$—are roughly 20 meV/atom higher, and subsequently, slightly closer to the LDA values.
[70] K. M. Myles, Trans. Metall. Soc. AIME **242**, 1523 (1968).
[71] N. Selhaoui, J. C. Gachon, and J. Hertz, J. Less Common Met. **154**, 137 (1989).
[72] J. C. Gachon, J. Phys. Chem. Solids **49**, 435 (1988).
[73] C. Wolverton and D. de Fontaine, Phys. Rev. B **49**, 12 351 (1994).